Eur. Phys. J. Spec. Top. (2022) 231:3629–3648
https://doi.org/10.1140/epjs/s11734-022-00534-5

THE EUROPEAN PHYSICAL JOURNAL SPECIAL TOPICS

Regular Article

The modeling and analysis of the COVID-19 pandemic with vaccination and treatment control: a case study of Maharashtra, Delhi, Uttarakhand, Sikkim, and Russia in the light of pharmaceutical and non-pharmaceutical approaches

Pankaj Singh Rana[a] and Nitin Sharma[b]

National Institute of Technology Uttarakhand, Srinagar (Garhwal) 246174, Uttarakhand, India

Received 25 January 2022 / Accepted 5 March 2022 / Published online 8 April 2022

Abstract Nonlinear dynamics is an exciting approach to describe the dynamical practices of COVID-19 disease. Mathematical modeling is a necessary method for investigating the dynamics of epidemic diseases. In the current article, an effort has been made to cultivate a novel COVID-19 compartment mathematical model by incorporating vaccinated populations. Primarily, the fundamental characteristics of the model, such as positivity and boundedness of solutions, are established. Thereafter, equilibrium analysis of steady states has been illustrated through vaccine reproduction number. Further, a nonlinear least square curve fitting technique has been employed to recognize the best fitted model parameters from the COVID-19 mortality data of five regions, namely Maharashtra, Delhi, Uttarakhand, Sikkim, and Russia. The numerical framework of the model has been added to interpret the consequence of various control schemes (pharmaceutical or non-pharmaceutical) on COVID-19 dynamics, and it has been ascertained that all the control protocols have a positive influence on curtailing the COVID-19 transference in the aforementioned regions. In addition, the essence of vaccine efficacy and vaccine-induced immunity are examined by considering different scenarios. Our analysis demonstrates that the disease will be wiped off from the Maharashtra, Delhi, Uttarakhand and Sikkim regions of India, while it shall persist in Russia for some more time. It is also found that, if a vaccine calamity arises, the government should majorly focus on permanent drug treatment of hospitalized individuals rather than vaccination.

Mathematics Subject Classification Primary 92B05 · Secondary 62P10

1 Introduction

The current coronavirus pandemic (COVID-19), caused by the highly contagious SARS-CoV-2 virus, is a devastating disease. Since its release from China's Wuhan City in December 2019, it has had unprecedented consequences that are causing massive crises all over the world [1]. Due to its deadly nature, the World Health Organization (WHO) announced it as a global pandemic on March 11, 2020 [2]. The nonlinear dynamics perspective of COVID-19 has attracted increasing attention since it contributes to the understanding of pandemic evolution. Hence, it is convenient and helpful in establishing the appropriate health strategy plans. A literature study revealed that SARS-CoV-2 originated from pangolins and bats [3]. The virus transmission can be through the droplets impending out from a cough or sneeze of a COVID-19 infected person. It is supposed that it can spread via direct contact with an infected individual or through indirect contact with contaminated objects [4]. The regular symptoms of COVID-19 include dry cough, fever, shortness of breath, fatigue, sore throat, and aches. According to the literature, the majority of infected people have mild to moderate symptoms and recover quickly without any specific treatment. Individuals who are suffering from comorbidity (having diabetes, cancer, chronic respiratory disease, etc.) or medical illness are more susceptible to infection than normal individuals [5].

During the second wave of COVID-19, it was detected that the reinfection rate was very sharp as compared to the first wave. In addition, the Indian Centre for Medical Research deliberated that the reinfection rate is 4.5% in the second wave of COVID-19 and that a

[a]e-mail: pankajsinghrana032@gmail.com
[b]e-mail: drnitinsharma@hotmail.com (corresponding author)

maximum of the reinfection cases are asymptomatic [6]. Governments come up with various types of intervention policies, such as enforcing complete lockdown and prolonging this lockdown for more time with relaxation and facial sanitization, wearing face masks, and maintaining social distancing as necessary. However, these policies assisted in a reduction of the infection rate but could not mitigate the disease completely [7]. The emergence of vaccinations magnified the optimism that the end of SARS-CoV-2 could be attainable. The immediate lockdown combined with rapid vaccination can improve the COVID-19 situation. Countries with a high vaccination rate are thought to have fewer active, fatal, and hospitalized cases on a daily basis.

A literature study showed that numerous forms of epidemiological models are employed to portray different epidemic diseases. An exciting and convenient approach is compartment modeling of the population. Kermack and Mckendrick [8] produced an epidemic model using three compartments: susceptible, infected, and recovered (SIR), which was further improved by Anderson [9] and May [10] by considering an extra compartment exposed. Nowadays, various epidemic models are established based on the susceptible, exposed, infected, and recovered (SEIR) framework, such as the influenza model, the HIV model, and the Zika model [11].

Currently, these models are largely used to designate COVID-19 dynamics. So that the disease transmission dynamics and its future behavior can be premeditated. Lin et al. [12] proposed a model for COVID-19 in Wuhan, China, contemplating individual behavior and government actions. Bastos et al. [13] used two variations of the SIR model for COVID-19 in Brazil and predicted the optimal date for mitigating the social distancing policy. Further, Mandal et al. [14] refined the SEIR model by including quarantine class and government intervention policy and predicted the disease dynamics in three eminently damaged states in India. Rai et al. [15] explained the SEIR model by considering the influence of social media advertising and deduced that social media awareness boosts the control of disease transmission. Gowrisankar et al. [16] analyzed the COVID-19 infection data from the top 15 affected countries, and moreover, their comparison results with other countries demonstrate that India has a lower death rate or more immunity against COVID-19. Thereafter, Easwaramoorthy et al. [17] introduced a fractal based prognostic model that compared and predicted the first and second waves of the COVID-19 pandemic in the five most affected countries: USA, Brazil, Russia, India, and the UK. Similarly, Kavitha et al. [18] applied the SIR and fractal interpolation methods to establish the trend of COVID-19 second and third waves in India and its provinces, namely Delhi, Karnataka, Tamil Nadu, Kerala, and Maharashtra. Furthermore, Khajanchi et al. [19] proposed a compartment model with nine stages of infection to control and forecast the pandemic situation in India. They also implemented an optimal control scheme considering pharmaceutical and non-pharmaceutical interventions as control functions. Their study determines that the implementation of both control schemes is more effective as compared to a single control scheme or no control scheme.

The influence of vaccination is often considered in epidemic models to illustrate disease control. Das et al. [20] formulated a COVID-19 model with comorbidity and claimed that disease will persist in society whenever exposed individuals have comorbidity. Moreover, they anticipate that disease can be controlled by utilizing proper non-pharmaceutical interventions and vaccination approaches. Similarly, Foy et al. [21] explored an age-structured deterministic SEIR model to assess age specific vaccine allocation tactics in India. Their findings suggest that older age groups (≥ 60) should be prioritized for vaccination over younger age groups to reduce disease-induced mortality.

In the absence of entire extinction schemes, the vaccination process has been considered the best remedy to protect humans from the COVID-19 infection globally. Therefore, it is instructive to practice the Mathematical Models to assess the potential effect of a hypothetical anti-COVID-19 vaccine. However, it is believed that SARS-CoV-2 will be finished once herd immunity has been acquired (naturally or through vaccination). But, the endemic model to evaluate the impact of the vaccination process on COVID-19 dynamics has to be established.

The present work deals with the novel deterministic model for the COVID-19 pandemic that portrays the disease transmission from symptomatic infected, asymptomatic infected, and vaccinated populations. The established model employed a system of seven differential equations to deal with the evolution of susceptible, vaccinated, exposed, asymptomatic, symptomatic, hospitalized, and recovered populations. Furthermore, the parameter estimation has been calculated by fitting our model to the daily reported deaths and cumulative deaths of COVID-19. In this regard, reported daily death data and cumulative death data from Maharashtra, Delhi, Uttarakhand, Sikkim, and Russia show good agreement between simulated outcomes and reported outcomes. The comprehensive stability analysis of equilibrium points is performed to investigate the qualitative behavior of the pandemic. Moreover, the effects of non-pharmaceutical interventions (i.e., lockdown) and pharmaceutical interventions (i.e., drug treatment, vaccination, and vaccine efficacy) on the five regions mentioned above are explored under different scenarios. Results demonstrate that nonlinear dynamics is an efficient tool to inspect COVID-19 pandemic evolution in any region.

2 Model development and assumptions

A nonlinear system of equations has been employed to classify the creation of a deterministic model for COVID-19. An additional vaccination population compartment has been included by assuming that recovery after vaccination is impermanent. The total popu-

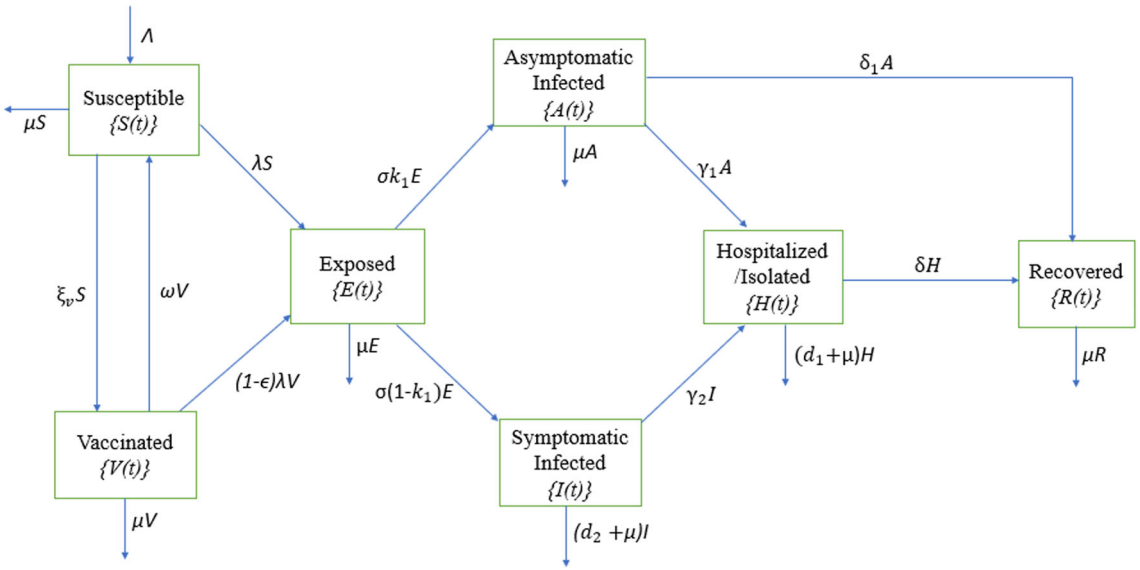

Fig. 1 Flow diagram of the model

lation $N(t)$ has been separated into seven distinct compartments, namely: susceptible $S(t)$; vaccinated $V(t)$; exposed $E(t)$; asymptomatic infected $A(t)$; symptomatic infected $I(t)$; hospitalized/isolated $H(t)$ and recovered $R(t)$, as shown in Fig. 1. Susceptible grasp infection from the individuals of asymptomatic class A and symptomatic infected I at λ rate (force of infection). Here, β is the disease transmission coefficient due to asymptomatic and symptomatic individuals. The modification parameter η_1 $(0 < \eta_1 \leq 1)$ defines that infection rate is faster in symptomatic individuals as compared to asymptomatic individuals. Susceptible individuals are vaccinated at ξ_v rate and $\epsilon(0 < \epsilon \leq 1)$ considered the vaccine efficacy for the protection of further infection from infected individuals. Further, ω measured the rate of loss of vaccine-induced immunity. Exposed individuals join the asymptomatic class and the symptomatic class with σk_1 and $(1-k_1)\sigma$ rates, respectively. The isolation or hospitalization rates for asymptomatic and symptomatic patients are signified by γ_1 and γ_2, respectively. While, recovery rate of isolated or hospitalized individuals is denoted by δ.

Some other adopted basic assumptions are listed as follows:

- Some portion of the susceptible individuals follow the COVID-19 guidelines of lockdown (wear facemasks, maintain social distance, etc.) and denoted by θ. Therefore, $(1-\theta)$ percentage of the population can contribute to the disease transmission. Hence, the disease transmission rate becomes $\beta(1-\theta)$.
- Vaccine-induced immunity is not eternal. Therefore, we applied the parameter ω to represent the rate of loss of vaccine-induced immunity.
- The COVID-19 vaccine is imperfect, so infection from vaccinated individuals can occur, but at a reduced rate as compared to infection from susceptible individuals.
- Some symptomatic individuals may die before being notified, so we assumed that they die at d_2 rate.
- Some hospitalized or isolated individuals may have severe COVID-19 infections that lead to deaths. Therefore, we presume d_1 a disease-induced death rate for hospitalized or isolated patients.
- Some vaccinated individuals may not be protected from infection, and therefore can infect others if they become infectious again.
- Some proportion of the asymptomatic class may recover naturally (without isolation) at δ_1 rate.
- $H(t)$ class contains individuals who are either hospitalized or isolated but are non-infectious.
- All the compartments have the same natural death rate expressed by μ.
- The disease-induced death rate for the asymptomatic class is negligible, hence not measured in the present model.

A model with governing nonlinear differential equations is defined as follows:

$$\begin{aligned}
\frac{\mathrm{d}S}{\mathrm{d}t} &= \Lambda - \lambda S + \omega V - (\xi_v + \mu) S \\
\frac{\mathrm{d}V}{\mathrm{d}t} &= \xi_v S - (1-\epsilon)\lambda V - (\omega + \mu) V \\
\frac{\mathrm{d}E}{\mathrm{d}t} &= \lambda S + (1-\epsilon)\lambda V - (\sigma + \mu) E \\
\frac{\mathrm{d}A}{\mathrm{d}t} &= \sigma k_1 E - (\mu + \gamma_1 + \delta_1) A \\
\frac{\mathrm{d}I}{\mathrm{d}t} &= \sigma(1-k_1) E - (\mu + \gamma_2 + d_2) I \\
\frac{\mathrm{d}H}{\mathrm{d}t} &= \gamma_1 A + \gamma_2 I - (\mu + d_1 + \delta) H \\
\frac{\mathrm{d}R}{\mathrm{d}t} &= \delta H + \delta_1 A - \mu R, \qquad (1)
\end{aligned}$$

where λ is the force of infection explained as follows:

$$\lambda = \frac{\beta(\eta_1 A + I)(1-\theta)}{N}.$$

3 Non-negativity and boundedness of solutions

To make our model biologically and epidemiologically well posed, non-negativity and boundedness of solutions are very imperative, which we shall verify in the following lemmas 1 and 2.

Lemma 1 *Let initially* $\{(S(0), V(0), E(0), A(0), I(0), H(0), R(0)) \in \boldsymbol{R}_+^7\}$ *then all the solutions of system Eq. (1) will remain positive for all* $t \geq 0$.

Proof Now, to prove the positivity of all solutions of system Eq. (1), we have:

$$\begin{aligned}
\left(\frac{dS}{dt}\right)_{S=0} &= \Lambda + \omega V \geq 0 \\
\left(\frac{dV}{dt}\right)_{V=0} &= \xi_v S \geq 0 \\
\left(\frac{dE}{dt}\right)_{E=0} &= \lambda S + (1-\epsilon)\lambda V \geq 0 \\
\left(\frac{dA}{dt}\right)_{A=0} &= \sigma k_1 E \geq 0 \\
\left(\frac{dI}{dt}\right)_{I=0} &= \sigma(1-k_1)E \geq 0 \\
\left(\frac{dH}{dt}\right)_{H=0} &= \gamma_1 A + \gamma_2 I \geq 0 \\
\left(\frac{dR}{dt}\right)_{R=0} &= \delta H + \delta_1 A \geq 0.
\end{aligned} \tag{2}$$

Equation (2) confirms that all the state variables are non-decreasing functions at any time. Further, since initially all the state variables are non-negative, it follows that state variables will be non-negative for all $t \geq 0$. Thus, the positivity of solutions has been clearly proven. □

Lemma 2 *The system Eq. (1) is bounded in the region* $\left(\Omega = \{S(t), V(t), E(t), A(t), I(t), H(t), R(t)\} \in \boldsymbol{R}_+^7 : N(t) \leq \frac{\Lambda}{\mu}\right)$.

Proof Since

$$N(t) = S(t) + V(t) + E(t) + A(t) + I(t) + H(t) + R(t)$$

implies

$$\frac{dN}{dt} = \frac{dS}{dt} + \frac{dV}{dt} + \frac{dE}{dt} + \frac{dA}{dt} + \frac{dI}{dt} + \frac{dH}{dt} + \frac{dR}{dt},$$

now substituting all the values from system Eq. (1), we have

$$\frac{dN}{dt} = \Lambda - \mu N - d_2 I - d_1 H \leq \Lambda - \mu N.$$

Now, we have following inequality:

$$\frac{dN}{dt} \leq \Lambda - \mu N$$

on integrating and using initial condition,

$$\begin{aligned}
0 \leq N(t) &\leq \frac{\Lambda}{\mu} + \left(N(0) - \frac{\Lambda}{\mu}\right) e^{-\mu t} \\
\limsup N(t) &\leq \frac{\Lambda}{\mu} \; as \; t \longrightarrow \infty.
\end{aligned}$$

Thus, the region Ω is positive invariant and bounded so no solution will pass beyond the boundary of Ω. □

4 Model system dynamics

4.1 Equilibrium analysis and the vaccine reproduction number

The model Eq. (1) has a unique disease-free equilibrium (DFE) point as

$$\begin{aligned}
E_0 &= (S_0, V_0, E_0, A_0, I_0, H_0, R_0) \\
&= \left(\frac{\Lambda(\omega+\mu)}{\mu(\xi_v+\omega+\mu)}, \frac{\Lambda\xi_v}{\mu(\xi_v+\omega+\mu)}, 0, 0, 0, 0, 0\right).
\end{aligned} \tag{3}$$

Now, to achieve the vaccine reproduction number (R_{0v}), next-generation matrix approach is used. Let the system Eq. (1) can be written as

$$\dot{x} = \mathcal{F}(x) - \mathcal{V}(x),$$

where matrix $\mathcal{F}$ corresponds to new infection terms, while matrix $\mathcal{V}$ corresponds to remaining transfer terms. Now, writing the model system variables in $x = (E, A, I, H)^T$ sequence, we have

$$\mathcal{F}(x) = \begin{bmatrix} \lambda S + (1-\epsilon)\lambda V \\ 0 \\ 0 \\ 0 \end{bmatrix},$$

$$\mathcal{V}(x) = \begin{bmatrix} (\sigma+\mu)E \\ (\mu+\gamma_1+\delta_1)A - \sigma k_1 E \\ (\mu+\gamma_2+d_2)I - \sigma(1-k_1)E \\ (\mu+d_1+\delta)H - \gamma_1 A - \gamma_2 I \end{bmatrix}.$$

Now, using Eq. (3) at disease-free equilibrium point, the Jacobian matrices F and V can be written as

$$F = \begin{bmatrix} 0 & \frac{\beta\eta_1(1-\theta)(S_0+(1-\epsilon)V_0)}{N_0} & \frac{\beta(1-\theta)(S_0+(1-\epsilon)V_0)}{N_0} & 0 \\ 0 & 0 & 0 & 0 \\ 0 & 0 & 0 & 0 \\ 0 & 0 & 0 & 0 \end{bmatrix}$$

$$V = \begin{bmatrix} m_1 & 0 & 0 & 0 \\ -\sigma k_1 & m_2 & 0 & 0 \\ -\sigma(1-k_1) & 0 & m_3 & 0 \\ 0 & -\gamma_1 & -\gamma_2 & m_4 \end{bmatrix},$$

where $m_1 = (\sigma+\mu)$, $m_2 = (\mu+\gamma_1+\delta_1)$, $m_3 = (\mu+\gamma_2+d_2)$, $m_4 = (\mu+d_1+\delta)$. Hence,

$$R_{0v} = \rho\left(FV^{-1}\right) = \frac{\beta\sigma(1-\theta)\left((1-k_1)m_2+\eta_1 k_1 m_3\right)(S_0+(1-\epsilon)V_0)}{m_1 m_2 m_3 N_0}. \tag{4}$$

At disease-free equilibrium point substituting the values of N_0, S_0, V_0 and m_1, m_2, m_3 in Eq. (4), we have

Basic reproduction number without vaccination is denoted by R_0 and written as the following equation:

$$R_0 = \frac{\beta\sigma(1-\theta)((1-k_1)(\mu+\gamma_1+\delta_1)+\eta_1 k_1(\mu+\gamma_2+d_2))}{(\sigma+\mu)(\mu+\gamma_1+\delta_1)(\mu+\gamma_2+d_2)} \tag{6}$$

implies

$$R_{0v} = R_0\left(\frac{(S_0+(1-\epsilon)V_0}{N_0}\right).$$

Now, substituting the values of N_0, S_0 and V_0, we get the relation between R_{0v} and R_0 as follows:

$$R_{0v} = R_0\left(1-\frac{\epsilon\xi_v}{(\xi_v+\omega+\mu)}\right). \tag{7}$$

4.2 Stability of equilibrium points

Theorem 1 *The disease-free equilibrium point* $\{E_0\}$ *is locally asymptotically stable for* $R_{0v} < 1$, *whereas unstable for* $R_{0v} > 1$.

Proof The Jacobian matrix J_{E_0} at disease-free equilibrium point will be

$$J_{E_0} = \begin{bmatrix} -(\xi_v+\mu) & \omega & 0 & \frac{-\beta\eta_1(1-\theta)S_0}{N_0} & \frac{-\beta(1-\theta)S_0}{N_0} & 0 & 0 \\ \xi_v & -(\omega+\mu) & 0 & \frac{-\beta\eta_1(1-\epsilon)(1-\theta)V_0}{N_0} & \frac{-\beta(1-\epsilon)(1-\theta)V_0}{N_0} & 0 & 0 \\ 0 & 0 & -(\sigma+\mu) & \frac{\beta\eta_1(1-\theta)(S_0+(1-\epsilon)V_0)}{N_0} & \frac{\beta(1-\theta)(S_0+(1-\epsilon)V_0)}{N_0} & 0 & 0 \\ 0 & 0 & \sigma k_1 & -(\mu+\gamma_1+\delta_1) & 0 & 0 & 0 \\ 0 & 0 & \sigma(1-k_1) & 0 & -(\mu+\gamma_2+d_2) & 0 & 0 \\ 0 & 0 & 0 & \gamma_1 & \gamma_2 & -(\mu+d_1+\delta) & 0 \\ 0 & 0 & 0 & \delta_1 & 0 & \delta & -\mu \end{bmatrix}.$$

$$N_0 = S_0 + V_0 = \frac{\Lambda}{\mu},\ S_0 = \frac{\Lambda(\omega+\mu)}{\mu(\xi_v+\omega+\mu)}\ and$$

The Jacobian matrix J_{E_0} has two eigen values as $-\mu$ and $-(\mu+d_1+\delta)$, and the other eigen values will be the eigen values of subsequent two block matrices J_{1E_0} and J_{2E_0}:

$$J_{1E_0} = \begin{bmatrix} -(\xi_v+\mu) & \omega \\ \xi_v & -(\omega+\mu) \end{bmatrix} \text{ and } J_{2E_0} = \begin{bmatrix} -(\sigma+\mu) & \frac{\beta\eta_1(1-\theta)(S_0+(1-\epsilon)V_0)}{N_0} & \frac{\beta(1-\theta)(S_0+(1-\epsilon)V_0)}{N_0} \\ \sigma k_1 & -(\mu+\gamma_1+\delta_1) & 0 \\ \sigma(1-k_1) & 0 & -(\mu+\gamma_2+d_2) \end{bmatrix}.$$

$$V_0 = \frac{\Lambda\xi_v}{\mu(\xi_v+\omega+\mu)}.$$

Hence, the vaccine reproduction number R_{0v} is defined in the following equation:

The eigen values of J_{1E_0} are $-\mu$ and $-(\xi_v+\omega+\mu)$, whereas the eigen values of J_{2E_0} can be determined by solving the following cubic characteristic polynomial:

$$R_{0v} = \frac{\beta\sigma(1-\theta)((1-k_1)(\mu+\gamma_1+\delta_1)+\eta_1 k_1(\mu+\gamma_2+d_2))((1-\epsilon)\xi_v+(\omega+\mu))}{(\sigma+\mu)(\mu+\gamma_1+\delta_1)(\mu+\gamma_2+d_2)(\xi_v+\omega+\mu)}. \tag{5}$$

$$A_0\lambda^3 + A_1\lambda^2 + A_2\lambda + A_3 = 0$$

$$A_0 = 1,\ A_1 = (\sigma + 3\mu + \gamma_1 + \gamma_2 + \delta_1 + d_2)$$

$$\begin{aligned} A_2 = {} & (\sigma+\mu)(\mu+\gamma_1+\delta_1) \\ & + (\mu+\gamma_1+\delta_1)(\mu+\gamma_2+d_2) \\ & + (\mu+\gamma_2+d_2)(\sigma+\mu) \\ & - \sigma\beta(1-\theta)(1-k_1+k_1\eta_1) \\ & \times \left(1 - \frac{\epsilon\xi_v}{(\xi_v+\omega+\mu)}\right) \end{aligned}$$

$$\begin{aligned} A_3 = {} & (\sigma+\mu)(\mu+\gamma_1+\delta_1) \\ & \times (\mu+\gamma_2+d_2) - \sigma\beta(1-\theta) \\ & \times((1-k_1)(\mu+\gamma_1+\delta_1) \\ & + \eta_1 k_1(\mu+\gamma_2+d_2)) \\ & \times \left(1 - \frac{\epsilon\xi_v}{(\xi_v+\omega+\mu)}\right). \end{aligned}$$

A_3 can be written as

$$A_3 = (\sigma+\mu)(\mu+\gamma_1+\delta_1)(\mu+\gamma_2+d_2)(1-R_{0v}). \tag{8}$$

It can be observed from Eq. (8) that $A_0 > 0$, $A_1 > 0$ and also $A_3 > 0$ whenever $\mathrm{R_{0v}} < 1$. Therefore, we need to illustrate that $A_2 > 0$.

Since $R_{0v} < 1$ implies

$$\frac{\beta\sigma(1-\theta)((1-k_1)(\mu+\gamma_1+\delta_1)+\eta_1k_1(\mu+\gamma_2+d_2))((1-\epsilon)\xi_v+(\omega+\mu))}{(\sigma+\mu)(\mu+\gamma_1+\delta_1)(\mu+\gamma_2+d_2)(\xi_v+\omega+\mu)} < 1$$

$$\frac{\beta\sigma(1-\theta)((1-\epsilon)\xi_v+(\omega+\mu))}{(\xi_v+\omega+\mu)} < \frac{(\sigma+\mu)(\mu+\gamma_1+\delta_1)(\mu+\gamma_2+d_2)}{((1-k_1)(\mu+\gamma_1+\delta_1)+\eta_1k_1(\mu+\gamma_2+d_2))}$$

$$\begin{aligned} A_2 = {} & (\sigma+\mu)(\mu+\gamma_1+\delta_1) + (\mu+\gamma_1+\delta_1)(\mu+\gamma_2+d_2) + (\mu+\gamma_2+d_2)(\sigma+\mu) \\ & - \sigma\beta(1-\theta)(1-k_1+k_1\eta_1)\left(1 - \frac{\epsilon\xi_v}{(\xi_v+\omega+\mu)}\right) \end{aligned}$$

also,

$(\sigma+\mu)(\mu+\gamma_1+\delta_1)+(\mu+\gamma_1+\delta_1)(\mu+\gamma_2+d_2)+(\mu+\gamma_2+d_2)(\sigma+\mu) > (\sigma+\mu)(\mu+\gamma_1+\delta_1)+(\mu+\gamma_2+d_2)(\sigma+\mu)$ implies

$$\begin{aligned} A_2 > {} & (\sigma+\mu)(\mu+\gamma_1+\delta_1) + (\mu+\gamma_2+d_2)(\sigma+\mu) \\ & - \sigma\beta(1-\theta)(1-k_1+k_1\eta_1)\left(1 - \frac{\epsilon\xi_v}{(\xi_v+\omega+\mu)}\right) \end{aligned}$$

$$\begin{aligned} A_2 > {} & (\sigma+\mu)(\mu+\gamma_1+\delta_1) + (\mu+\gamma_2+d_2)(\sigma+\mu) \\ & - \frac{(1-k_1+k_1\eta_1)(\sigma+\mu)(\mu+\gamma_1+\delta_1)(\mu+\gamma_2+d_2)}{((1-k_1)(\mu+\gamma_1+\delta_1)+\eta_1k_1(\mu+\gamma_2+d_2))} \end{aligned}$$

$$\begin{aligned} A_2 > {} & \frac{(\sigma+\mu)((1-k_1)(\mu+\gamma_1+\delta_1)^2+\eta_1k_1(\mu+\gamma_2+d_2)^2)}{((1-k_1)(\mu+\gamma_1+\delta_1)+\eta_1k_1(\mu+\gamma_2+d_2))} \\ & > 0. \end{aligned}$$

Hence, using Routh–Hurwitz criterion, all the eigen values of Jacobian matrix J_{2E_0} are having negative real part, whenever $R_{0v} < 1$ and $A_1A_2 > A_3$. While if $R_{0v} > 1$ then $A_3 < 0$ implies, J_{2E_0} will have at least one eigenvalue with positive real part. Hence, DFE $\{E_0\}$ of the system is locally asymptotically stable when $R_{0v} < 1$ and unstable if $R_{0v} > 1$. □

Theorem 2 *The disease-free equilibrium point is globally stable whenever $R_{0v} \le 1$ in its feasible region Ω.*

Proof Now, to show the global stability of DFE, we used the Lyapunov function method. Let us construct a Lyapunov function as

$$\begin{aligned} & F\{S(t), V(t), E(t), A(t), I(t), H(t), R(t)\} \\ & \quad \to R_+ \text{ as} \\ & \quad F = E + g_1A + g_2I, \end{aligned}$$

where g_1 *and* g_2 are positive constants.

Taking time derivative of F, we get

$$\frac{\mathrm{d}F}{\mathrm{d}t} = \frac{\mathrm{d}E}{\mathrm{d}t} + g_1\frac{\mathrm{d}A}{\mathrm{d}t} + g_2\frac{\mathrm{d}I}{\mathrm{d}t}.$$

Now, substituting the values of $\frac{\mathrm{d}E}{\mathrm{d}t}$, $\frac{\mathrm{d}A}{\mathrm{d}t}$ *and* $\frac{\mathrm{d}I}{\mathrm{d}t}$ from model system Eq. (1), we have

$$\begin{aligned} \dot{F} = {} & \lambda S + (1-\epsilon)\lambda V - (\sigma+\mu)E \\ & + g_1\{\sigma k_1 E - (\mu+\gamma_1+\delta_1)A\} \\ & + g_2\{\sigma(1-k_1)E - (\mu+\gamma_2+d_2)I\} \end{aligned}$$

$$\begin{aligned} \dot{F} = {} & \frac{\beta(\eta_1A+I)(1-\theta)}{N}(S+(1-\epsilon)V) - (\sigma+\mu)E \\ & + g_1\{\sigma k_1E - (\mu+\gamma_1+\delta_1)A\} \\ & + g_2\{\sigma(1-k_1)E - (\mu+\gamma_2+d_2)I\}. \end{aligned}$$

At disease-free equilibrium point, we have from Eq. (3)

$$N_0 = S_0 + V_0 = \frac{\Lambda}{\mu},\ S_0 = \frac{\Lambda(\omega+\mu)}{\mu(\xi_v+\omega+\mu)} \quad \text{and}$$

$$V_0 = \frac{\Lambda\xi_v}{\mu(\xi_v+\omega+\mu)}$$

implies $\dot{F}$ can be written as

$$\dot{F} \le \frac{\beta(\eta_1A+I)(1-\theta)}{N}(S_0+(1-\epsilon)V_0) - (\sigma+\mu)E$$

$$
\begin{aligned}
&+g_1\left\{\sigma k_1 E-(\mu+\gamma_1+\delta_1)A\right\}\\
&+g_2\sigma(1-k_1)E-(\mu+\gamma_2+d_2)I\\
\dot{F}\leq\ &\beta(\eta_1 A+I)(1-\theta)\\
&\times\left(1-\frac{\epsilon\xi_v}{(\xi_v+\omega+\mu)}\right)-(\sigma+\mu)E\\
&+g_1\left\{\sigma k_1 E-(\mu+\gamma_1+\delta_1)A\right\}+g_2\{\sigma(1-k_1)E\\
&-(\mu+\gamma_2+d_2)I\}\\
\dot{F}\leq\ &[\sigma g_1 k_1+\sigma g_2(1-k_1)-(\sigma+\mu)]E\\
&+\left[\beta\eta_1(1-\theta)\left(1-\frac{\epsilon\xi_v}{(\xi_v+\omega+\mu)}\right)\right.\\
&\left.-g_1(\mu+\gamma_1+\delta_1)\right]A\\
&+\left[\beta(1-\theta)\left(1-\frac{\epsilon\xi_v}{(\xi_v+\omega+\mu)}\right)\right.\\
&\left.-g_2(\mu+\gamma_2+d_2)\right]I.
\end{aligned}
$$

Choose g_1 and g_2 such that

$$
\begin{aligned}
g_1&=\frac{\beta\eta_1(1-\theta)}{(\mu+\gamma_1+\delta_1)}\left(1-\frac{\epsilon\xi_v}{(\xi_v+\omega+\mu)}\right),\\
g_2&=\frac{\beta(1-\theta)}{(\mu+\gamma_2+d_2)}\left(1-\frac{\epsilon\xi_v}{(\xi_v+\omega+\mu)}\right)
\end{aligned}
$$

implies

$$
\begin{aligned}
\dot{F}\leq\ &\left[\frac{\sigma k_1\beta\eta_1(1-\theta)}{(\mu+\gamma_1+\delta_1)}\left(1-\frac{\epsilon\xi_v}{(\xi_v+\omega+\mu)}\right)\right.\\
&+\frac{\sigma\beta(1-k_1)(1-\theta)}{(\mu+\gamma_2+d_2)}\left(1-\frac{\epsilon\xi_v}{(\xi_v+\omega+\mu)}\right)\\
&\left.-(\sigma+\mu)\right]E\\
\dot{F}\leq\ &\left[\sigma\beta(1-\theta)\left(1-\frac{\epsilon\xi_v}{(\xi_v+\omega+\mu)}\right)\left(\frac{k_1\eta_1}{(\mu+\gamma_1+\delta_1)}\right.\right.\\
&\left.\left.+\frac{(1-k_1)}{(\mu+\gamma_2+d_2)}\right)-(\sigma+\mu)\right]E\\
\dot{F}\leq\ &(\sigma+\mu)\left[\frac{\sigma\beta(1-\theta)}{(\sigma+\mu)}\left(1-\frac{\epsilon\xi_v}{(\xi_v+\omega+\mu)}\right)\right.\\
&\left.\times\left(\frac{k_1\eta_1}{(\mu+\gamma_1+\delta_1)}+\frac{(1-k_1)}{(\mu+\gamma_2+d_2)}\right)-1\right]E\\
\dot{F}\leq\ &(\sigma+\mu)(R_{0v}-1)E. \qquad (9)
\end{aligned}
$$

Hence, it can be clearly verified from Eq. (9) that $\dot{F}\leq 0$ if $R_{0v}\leq 1$ and $\dot{F}=0$ if and only if either $R_{0v}=1$ or $E=0$; now, put $E=0$ in system Eq. (1), we have $S\to S_0, V\to V_0, A\to 0, I\to 0, H\to 0, R\to 0$ as $t\to\infty$. Thus, maximal invariant set in $\{(S(t),V(t),E(t),A(t),I(t),H(t),R(t))\,\epsilon\,\Omega:\dot{F}=0\}$ is singleton DFE $\{E_0\}$ if $R_{0v}\leq 1$. Hence, by La Salle invariance principle [22], $\{E_0\}$ is globally stable if $R_{0v}\leq 1$. □

Pandemic equilibrium point analysis

Pandemic equilibrium point can be found by solving the following system equations:

$$
\begin{aligned}
&\Lambda-\lambda S+\omega V-(\xi_v+\mu)S=0\\
&\xi_v S-(1-\epsilon)\lambda V-(\omega+\mu)V=0\\
&\lambda S+(1-\epsilon)\lambda V-(\sigma+\mu)E=0\\
&\sigma k_1 E-(\mu+\gamma_1+\delta_1)A=0\\
&\sigma(1-k_1)E-(\mu+\gamma_2+d_2)I=0\\
&\gamma_1 A+\gamma_2 I-(\mu+d_1+\delta)H=0\\
&\delta H+\delta_1 A-\mu R=0, \qquad (10)
\end{aligned}
$$

we get pandemic equilibrium point $E_e^*=(S^*,V^*,E^*,A^*,I^*,H^*,R^*)$ determined as follows:

$$
\begin{aligned}
S^*&=\frac{\Lambda\{(1-\epsilon)\lambda+(\omega+\mu)\}}{[(\lambda+\xi_v+\mu)\{(1-\epsilon)\lambda+(\omega+\mu)\}-\omega\xi_v]}\\
V^*&=\frac{\Lambda\xi_v}{[(\lambda+\xi_v+\mu)\{(1-\epsilon)\lambda+(\omega+\mu)\}-\omega\xi_v]}\\
E^*&=\frac{\lambda}{(\sigma+\mu)}\left(S^*+(1-\epsilon)V^*\right),\ A^*=\frac{\sigma k_1 E^*}{(\mu+\gamma_1+\delta_1)},\\
I^*&=\frac{\sigma(1-k_1)E^*}{(\mu+\gamma_2+\delta_2)},\ H^*=\frac{\gamma_1 A^*+\gamma_2 I^*}{(\mu+d_1+\delta)},\\
R^*&=\frac{\delta H^*+\delta_1 A^*}{\mu}.
\end{aligned}
$$

Similarly, applying the same Lyapunov function, we established the stability of pandemic equilibrium point of the system Eq. (1), which consequently states the following result.

Theorem 3 *The Pandemic equilibrium point* $\{E_e^*\}$ *is globally asymptotically stable whenever* $R_{0v}>1$.

Proof For this, we have created the Lyapunov function L as follows:

$L:\{(S^*,V^*,E^*,A^*,I^*,H^*,R^*)\in\Omega^*\}\to\mathbb{R}$, where $\Omega^*=\{(S^*,V^*,E^*,A^*,I^*,H^*,R^*)\in\mathbb{R}^7: S(t),V(t),E(t),A(t),I(t),H(t),R(t)>0\}$

$$
\begin{aligned}
L=\ &C_1\left\{\mathrm{S}-\mathrm{S}^*\ln\left(\frac{\mathrm{S}}{\mathrm{S}^*}\right)\right\}+C_2\left\{V-V^*\ln\left(\frac{V}{V^*}\right)\right\}\\
&+C_3\left\{E-E^*\ln\left(\frac{E}{E^*}\right)\right\}\\
&+C_4\left\{A-A^*\ln\left(\frac{A}{A^*}\right)\right\}\\
&+C_5\left\{I-I^*\ln\left(\frac{I}{I^*}\right)\right\}\\
&+C_6\left\{H-H^*\ln\left(\frac{H}{H^*}\right)\right\}\\
&+C_7\left\{R-R^*\ln\left(\frac{R}{R^*}\right)\right\}\\
\frac{\mathrm{d}L}{\mathrm{d}t}=\ &C_1(S-S^*)\frac{\mathrm{d}S}{\mathrm{d}t}+C_2(V-V^*)\frac{\mathrm{d}V}{\mathrm{d}t}
\end{aligned}
$$

$$+ C_3 (E - E^*) \frac{dE}{dt} + C_4 (A - A^*) \frac{dA}{dt} + C_5 (I - I^*) \frac{dI}{dt} + C_6 (H - H^*) \frac{dH}{dt} + C_7 (R - R^*) \frac{dR}{dt}.$$

Now, put down the values of derivatives from system Eq. (1), we have

$$\begin{aligned}\frac{dL}{dt} &= C_1 (S - S^*) \{\Lambda - \lambda S + \omega V - (\xi_v + \mu) S\} \\ &+ C_2 (V - V^*) \{\xi_v S - (1 - \epsilon) \lambda V - (\omega + \mu) V\} \\ &+ C_3 (E - E^*) \{\lambda S + (1 - \epsilon) \lambda V - (\sigma + \mu) E\} \\ &+ C_4 (A - A^*) \{\sigma k_1 E - (\mu + \gamma_1 + \delta_1) A\} \\ &+ C_5 (I - I^*) \{\sigma (1 - k_1) E - (\mu + \gamma_2 + d_2) I\} \\ &+ C_6 (H - H^*) \{\gamma_1 A + \gamma_2 I - (\mu + d_1 + \delta) H\} \\ &+ C_7 (R - R^*) \{\delta H + \delta_1 A - \mu R\}. \end{aligned} \tag{11}$$

Now, at pandemic equilibrium point,

$$\begin{aligned}\Lambda &= \frac{\beta (1 - \theta) (n_1 A^* + I^*)}{N} S^* - (\xi_v + \mu) S^* + \omega V^*, \\ \xi_v S^* &= (1 - \epsilon) \frac{\beta (1 - \theta) (n_1 A^* + I^*) V^*}{N} - (\omega + \mu) V^*, \\ (\sigma + \mu) E^* &= \frac{\beta (1 - \theta) (n_1 A^* + I^*)}{N} S^* + (1 - \epsilon) \\ &\quad \times \frac{\beta (1 - \theta) (n_1 A^* + I^*) V^*}{N}, \\ \sigma k_1 E^* &= (\mu + \gamma_1 + \delta_1) A^*, \sigma (1 - k_1) E^* \\ &= (\mu + \gamma_2 + d_2) I^*, \gamma_1 A^* + \gamma_2 I^* \\ &= (\mu + d_1 + \delta) H^*, \delta H^* + \delta_1 A^* = \mu R^*, \end{aligned}$$

using these conditions in Eq. (11), we get $\frac{dL}{dt} = -\mu \left(1 - \frac{S^*}{S}\right)^2 + \hat{f}(S, V, E, A, I, H, R)$,

where $\hat{f}(S, V, E, A, I, H, R)$ is non-positive by following the defined approach [23]. This implies $\hat{f} \leq 0$ for every $S, V, E, A, I, H, R > 0$. We found that $\frac{dL}{dt} \leq 0$ and $\frac{dL}{dt} = 0$ only if $S = S^*, V = V^*, E = E^*, A = A^*, I = I^*, H = H^*, R = R^*$. Thus, pandemic equilibrium point $\{E_e^*\}$ is the only singleton set for which $\frac{dL}{dt} = 0$. Applying LaSalle invariance principal, it can be verified that $\{E_e^*\}$ is globally asymptotically stable whenever $R_{0v} > 1$. □

5 Model parameter estimation and vaccine reproduction number

The novel COVID-19 model has been employed to accomplish dynamical analysis of the pandemic. We have elected four states of India, namely Maharashtra, Delhi, Uttarakhand and Sikkim, and a majorly affected country named Russia. Russia has been chosen to validate our model for its application in other countries. Our model uses reported death data from novel COVID-19 in Maharashtra, Delhi, Uttarakhand, Sikkim, and Russia to demonstrate its ability to predict different COVID-19 scenarios. The fixed demographic parameters and initial conditions for fitting the model are presented in Tables 2, 3, 4, 5, and 6 for Maharashtra, Delhi, Uttarakhand, Sikkim, and Russia, respectively. Daily new deaths of COVID-19 and cumulative deaths in Maharashtra [24], Delhi [25], Uttarakhand [26], Sikkim [27] and Russia [28] for the time period ranging from July 1st, 2021 to September 8th, 2021 are considered for study. The reason for using death data is that it is more reliable than the number of infected cases arising on daily basis. This is due to the limited testing capacities [29]. We fitted the model output ($\int_{t=1}^{T} (d_1 H + d_2 I)\, dt$ where T = 70) to the cumulative deaths and daily new deaths due to COVID-19. Eight unknown model parameters, namely $\beta, \gamma_1, \gamma_2, \delta, \delta_1, d_1, \omega, \xi_v$ and the initial number of exposed people, $E(0)$ are estimated from the reported mortality data [24–28]. During the specified time period, the nonlinear least square solver *lsqnonlin* of MATLAB has been applied to fit the simulated daily mortality data to the reported daily new deaths in the aforementioned five regions. The estimated parameters for these five regions are specified in Table 7. The fitting of daily deaths of COVID-19 and cumulative deaths of Maharashtra is displayed in Fig. 2a, and the same is depicted in Fig. 2b–e, for Delhi, Uttarakhand, Sikkim and Russia, respectively. It is clearly visible that fitting shows good agreement for all the regions between the numerical simulation and reported data.

The vaccine reproduction number is interpreted as the expected number of secondary infections caused by an infectious during its entire infectious period in a population. For our mathematical model, it is given in Eq. (5). We evaluated R_{0v} using estimated and fixed parameter values from Tables 2, 3, 4, 5, 6, and 7 for the aforementioned regions, namely Maharashtra, Delhi, Uttarakhand, Sikkim, and Russia, and listed them in Table 1.

6 Numerical results and case study analysis

We simulated the proposed model system Eq. (1) for Maharashtra, Delhi, Uttarakhand, Sikkim, and Russia by employing the parameter values and initial conditions from Tables 2, 3, 4, 5, 6 and 7 to measure the impact of pharmaceutical and non-pharmaceutical control interventions on the transmission of COVID-19.

6.1 The effects of drug treatment

Recently, several drugs have been discovered to have a quicker recovery from COVID-19. Such as the drug 2-deoxy-D-glucose (2-DG) originated by the "Institute of Nuclear Medicine and Allied Sciences (INMAS-DRDO)", in collaboration with Dr Reddy's Laborato-

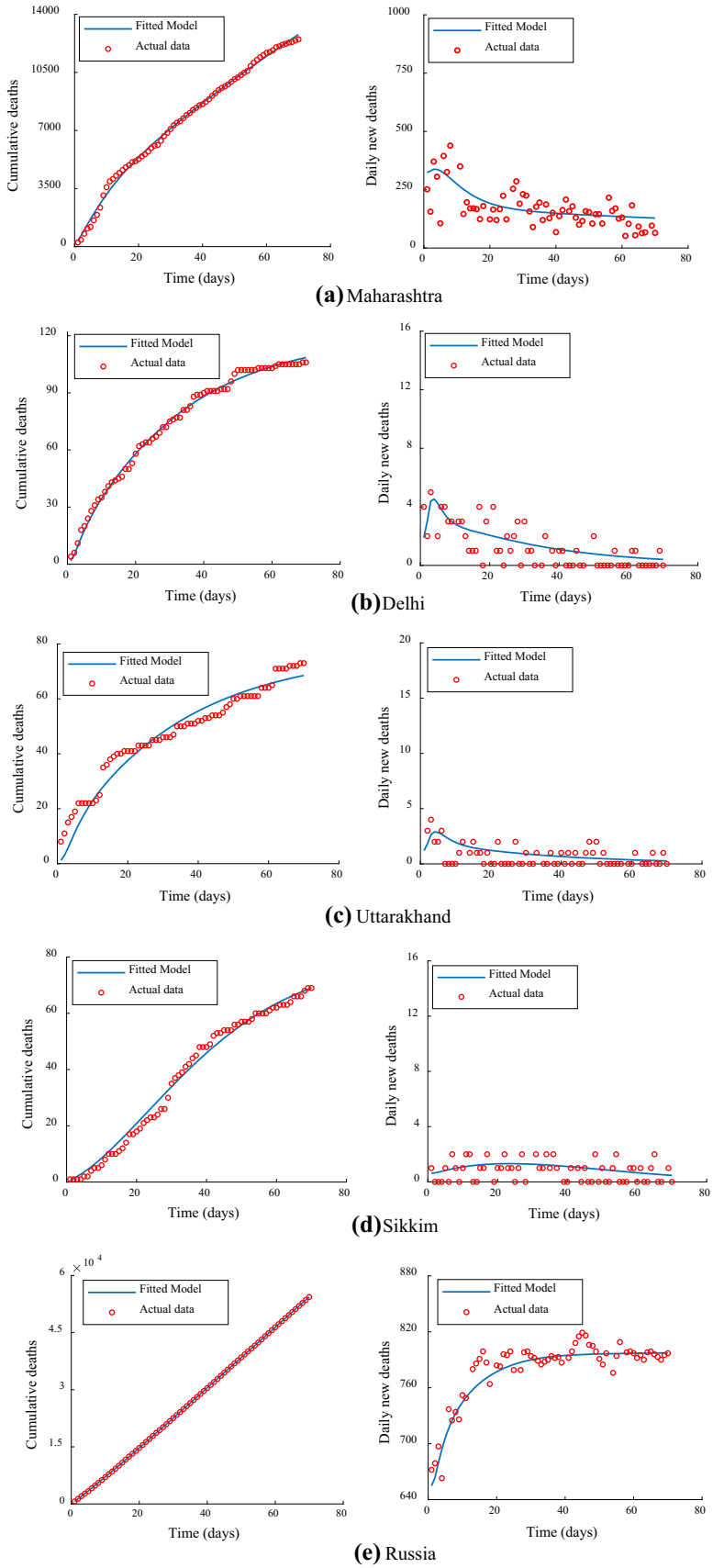

Fig. 2 Model fitting of reported COVID-19 data

Table 1 Calculated values of the vaccine reproduction number (R_{0v})

Region	Vaccine reproduction number ($\boldsymbol{R_{0v}}$)
Maharashtra	0.728828
Delhi	0.238979
Uttarakhand	0.275416
Sikkim	0.310588
Russia	1.00982

Table 2 Fixed parameter values and initial conditions for Maharashtra

Parameter/initial condition's	Description	Value	Source
$N(0)$	Initial population size	124904071	[30]
Λ	Recruitment rate	$\mu \times N(0)$	[31]
σ	Rate at which exposed class goes to infected class	0.2	[31]
k_1	Proportion of exposed class, who joins A class	0.3785	[32]
d_2	Disease induced mortality rate for symptomatic class	0.0052	[33]
μ	Natural mortality rate	3.914×10^{-5}	[34]
ϵ	Vaccine efficacy	0.8	[35]
η_1	Modification parameter	0.75	[36]
θ	Proportion of the population following intervention policies	0.6	Assumed
$S(0)$	Initial number of susceptible individuals	87432849	[37]
$V(0)$	Initial number of vaccinated individuals	30000	–
$E(0)$	Initial number of exposed individuals	22333	Estimated
$A(0)$	Initial number of asymptomatic individuals	30000	–
$I(0)$	Initial number of symptomatic individuals	9195	[24]
$H(0)$	Initial number of hospitalized individuals	15000	–
$R(0)$	Initial number of recovered individuals	50000	–

Table 3 Fixed parameter values and initial conditions for Delhi

Parameter/initial condition's	Description	Value	Source
$N(0)$	Initial population size	19301096	[38]
Λ	Recruitment rate	$\mu \times N(0)$	[31]
σ	Rate at which exposed class goes to infected class	0.2	[31]
k_1	Proportion of exposed class, who joins A class	0.3785	[32]
d_2	Disease induced mortality rate for symptomatic class	0.0052	[33]
μ	Natural mortality rate	3.914×10^{-5}	[34]
ϵ	Vaccine efficacy	0.8	[35]
η_1	Modification parameter	0.75	[36]
θ	Proportion of the population following intervention policies	0.6	Assumed
$S(0)$	Initial number of susceptible individuals	13510767	[37]
$V(0)$	Initial number of vaccinated individuals	500	–
$E(0)$	Initial number of exposed individuals	175	Estimated
$A(0)$	Initial number of asymptomatic individuals	500	–
$I(0)$	Initial number of symptomatic individuals	93	[25]
$H(0)$	Initial number of hospitalized individuals	15	–
$R(0)$	Initial number of recovered individuals	1000	–

ries (DRL), Hyderabad, and also approved by the drug controller general of India (DCGI) [46,47]. Its clinical trial demonstrated that this drug is very beneficial in hastening the recovery of hospitalized patients and also in reducing the need for supplemental oxygen.

The mild symptomatic and asymptomatic classes do not need intensive treatment. Therefore, antiviral drug treatment is implemented only for hospitalized patients. We considered that the recovery rate of hospitalized patients through antiviral drug treatment is represented by δ. According to Fig. 3a–e, when antiviral drugs are unavailable ($\delta = 0$), the hospitalized population peaks in Maharashtra, Delhi, Uttarakhand, Sikkim, and Russia. When the treatment rate differs over time, the hospitalized population assumes bigger values at the beginning of an outbreak. While increasing the treatment

Table 4 Fixed parameter values and initial conditions for Uttarakhand

Parameter/initial condition's	Description	Value	Source
$N(0)$	Initial population size	11700099	[39]
Λ	Recruitment rate	$\mu \times N(0)$	[31]
σ	Rate at which exposed class goes to infected class	0.2	[31]
k_1	Proportion of exposed class, who joins A class	0.3785	[32]
d_2	Disease induced mortality rate for symptomatic class	0.0052	[33]
μ	Natural mortality rate	3.914×10^{-5}	[34]
ϵ	Vaccine efficacy	0.8	[35]
η_1	Modification parameter	0.75	[36]
θ	Proportion of the population following intervention policies	0.6	Assumed
$S(0)$	Initial number of susceptible individuals	8190069	[37]
$V(0)$	Initial number of vaccinated individuals	500	–
$E(0)$	Initial number of exposed individuals	105	Estimated
$A(0)$	Initial number of asymptomatic individuals	500	–
$I(0)$	Initial number of symptomatic individuals	124	[26]
$H(0)$	Initial number of hospitalized individuals	15	–
$R(0)$	Initial number of recovered individuals	1000	–

Table 5 Fixed parameter values and initial conditions for Sikkim

Parameter/initial condition's	Description	Value	Source
$N(0)$	Initial population size	658019	[40]
Λ	Recruitment rate	$\mu \times N(0)$	[31]
σ	Rate at which exposed class goes to infected class	0.2	[32]
k_1	Proportion of exposed class, who joins A class	0.3785	[32]
d_2	Disease induced mortality rate for symptomatic class	0.0052	[33]
μ	Natural mortality rate	3.914×10^{-5}	[34]
ϵ	Vaccine efficacy	0.8	[35]
η_1	Modification parameter	0.75	[36]
θ	Proportion of population follow the intervention policies	0.6	Assumed
$S(0)$	Initial number of susceptible individuals	460613	[37]
$V(0)$	Initial number of vaccinated individuals	500	–
$E(0)$	Initial number of exposed individuals	100	Estimated
$A(0)$	Initial number of asymptomatic individuals	500	–
$I(0)$	Initial number of symptomatic individuals	122	[27]
$H(0)$	Initial number of hospitalized individuals	15	–
$R(0)$	Initial number of recovered individuals	1000	–

Table 6 Fixed parameter values and initial conditions for Russia

Parameter/initial condition's	Description	Value	Source
$N(0)$	Initial population size	145934462	[41]
Λ	Recruitment rate	$\mu \times N(0)$	[31]
σ	Rate at which exposed class goes to infected class	0.19608	[42]
k_1	Proportion of exposed class, who joins A class	0.5	[42]
d_2	Disease induced mortality rate for symptomatic class	0.0132	[43]
μ	Natural mortality rate	3.75×10^{-5}	[44]
ϵ	Vaccine efficacy	0.91	[45]
η_1	Modification parameter	0.5	[42]
θ	Proportion of population follow the intervention policies	0.6	Assumed
$S(0)$	Initial number of susceptible individuals	102154123	[37]
$V(0)$	Initial number of vaccinated individuals	50000	–
$E(0)$	Initial number of exposed individuals	39915	Estimated
$A(0)$	Initial number of asymptomatic individuals	50000	–
$I(0)$	Initial number of symptomatic individuals	23543	[28]
$H(0)$	Initial number of hospitalized individuals	20000	–
$R(0)$	Initial number of recovered individuals	70000	–

Table 7 Estimated parameter values for Uttarakhand, Maharashtra, Delhi, Sikkim, and Russia

Parameter	Description	Values Uttarakhand	Values Maharashtra	Values Delhi	Values Sikkim	Values Russia
β	Transmission coefficient	0.2176	0.2461	0.2124	0.4633	0.2799
γ_1	Rate at which asymptomatic individuals got hospitalized	0.0992	0.0841	0.0836	0.000003553	0.0001904
δ_1	Natural recovery rate of asymptomatic	0.32	0.2457	0.5677	0.3884	0.6312
δ	Recovery rate of hospitalized class after antiviral drug treatment	0.3699	0.1393	0.3340	0.0784	0.0692
γ_2	Rate at which infected individuals got hospitalized	0.0379	0.0124	0.0405	0.077	0.0014
d_1	Disease induced mortality rate for hospitalized class	0.0369	0.0184	0.0944	0.00010033	0.0172
ξ_v	Vaccination rate for susceptible	0.5133	0.5605	0.3285	0.0329	0.0818
ω	Rate of loss of vaccine-induced immunity	0.0063347	0.0036	0.000214	0.0000000735	0.0189

rate above zero, we see decrement in the hospitalized population. However, it should be pointed out that the recovered population presents the same trend of increment for all the regions with increasing treatment rates. The scenario recommends that treatment with drugs like 2-DG can be consumed to avoid high contamination of disease.

6.2 Vaccination's impact

Vaccination is a prominent tool for pharmaceutical interventions that decrease the number of susceptible individuals, thus reduces the disease in any population. We introduced a vaccination compartment in the proposed model and speculated that completion of vaccine doses implies only temporary immunity, and due to loss of immunity, individuals can re-join the susceptible class. Presently, several vaccines (Covaxin, Covishield, Sputnik, etc.) are being used by the government to combat COVID -19. We adopted the symbol ξ_v to know the effect of vaccination on the population, which demonstrates the vaccination rate in susceptible populations. Further, we considered that the vaccinated class contains those susceptible who are fully vaccinated and even completed 14 days after the last dose. Five different scenarios are considered for the effect of the vaccination rate $\xi_v = 0, 0.25, 0.5, 0.75, 1$. Figure 4a–e shows the impact of vaccination on the evolution of the pandemic in Maharashtra, Delhi, Uttarakhand, Sikkim, and Russia, respectively, expressing that vaccination has a huge impact on COVID-19. Higher the vaccination rate ξ_v, results lower the contamination peak and as well as the symptomatic and hospitalized population. As expected, the vaccination yields approximately the same deduction for all regions; in the absence of vaccination, disease will stay in the population forever.

6.3 The influence of vaccine efficacy

The efficacy of the vaccine plays an imperative role in the termination of COVID-19 infection. A symbol $\epsilon, (0 \leq \epsilon \leq 1)$ has been introduced to signify the vaccine efficacy to rescue people from COVID-19 infection. However, all the vaccines give some significant benefits in comparison to having no vaccine. Figure 5a–e clearly demonstrates that increasing the vaccine efficacy, results drop in infection peak as well as in symptomatic and hospitalized populations in Maharashtra, Delhi, Uttarakhand, Sikkim, and Russia, respectively. In addition, it can be detected for all five regions that whenever vaccine efficacy is zero, the disease will stay in the population, while whenever the vaccine is either fully or at least seventy five percent effective, the disease can be eliminated from the population provided other interventions work properly.

6.4 The influence of vaccine-induced immunity

Herd immunity refers to a group of susceptible individuals who are immune to infection and, as a result, can aid in the elimination of disease transmission. There are two ways to attain herd immunity. One is through natural immunity and the other is vaccine-induced immunity, although the latter is the most reliable and quickest way. Furthermore, individuals who are pregnant, undergoing medical implications, due to age restrictions or for some other reason, may be incapable of vaccinating against COVID-19. In this case, we used the parameter ω to depict vaccine-induced immunity, which ($\omega = 0$) expresses long-term immunity against infection.

Similarly, $\omega = 0.1 = 1/10$ implies 10 days of immunity from infection. Figure 6a–e clearly illustrates that when vaccine-induced immunity is permanent, symptomatic and hospitalized cases can be reduced rapidly

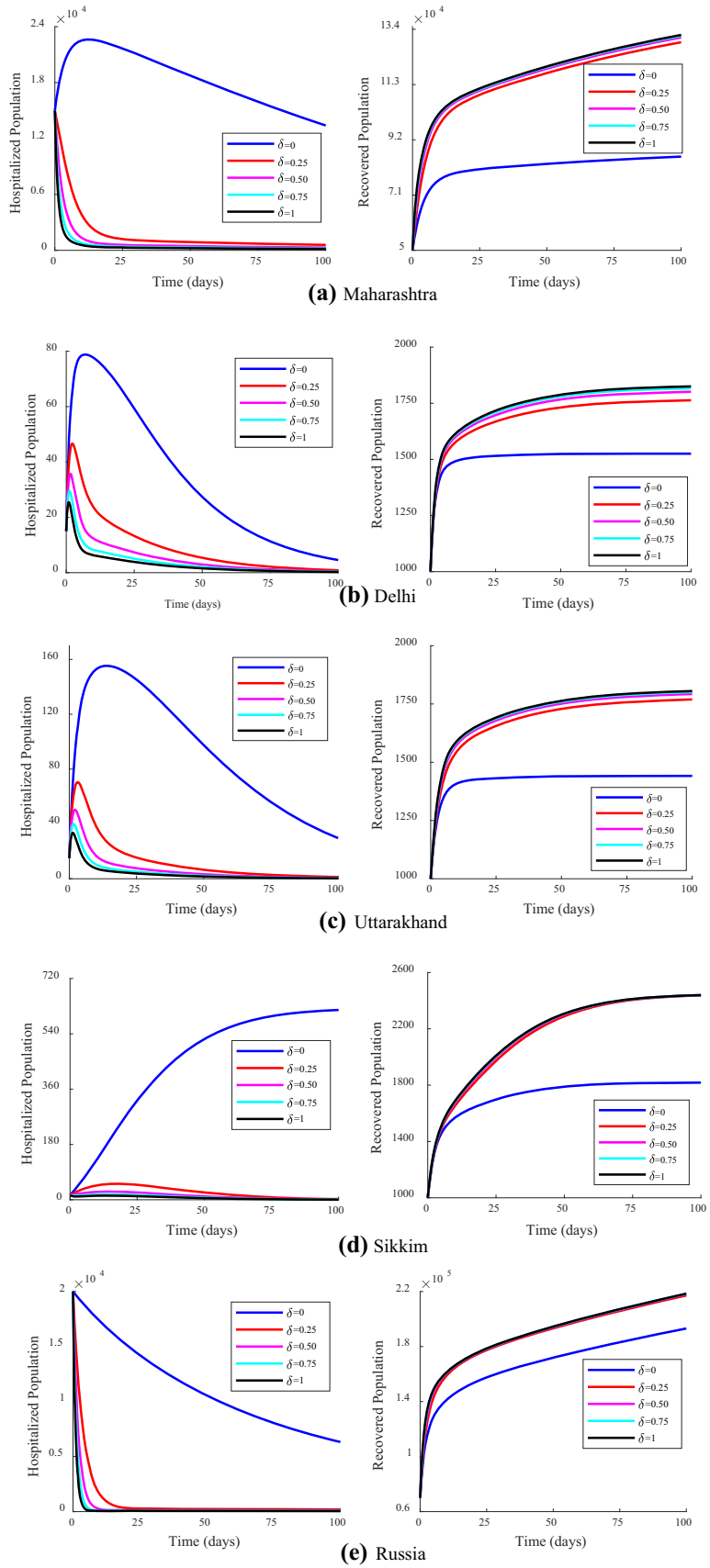

Fig. 3 Effect of drug treatment

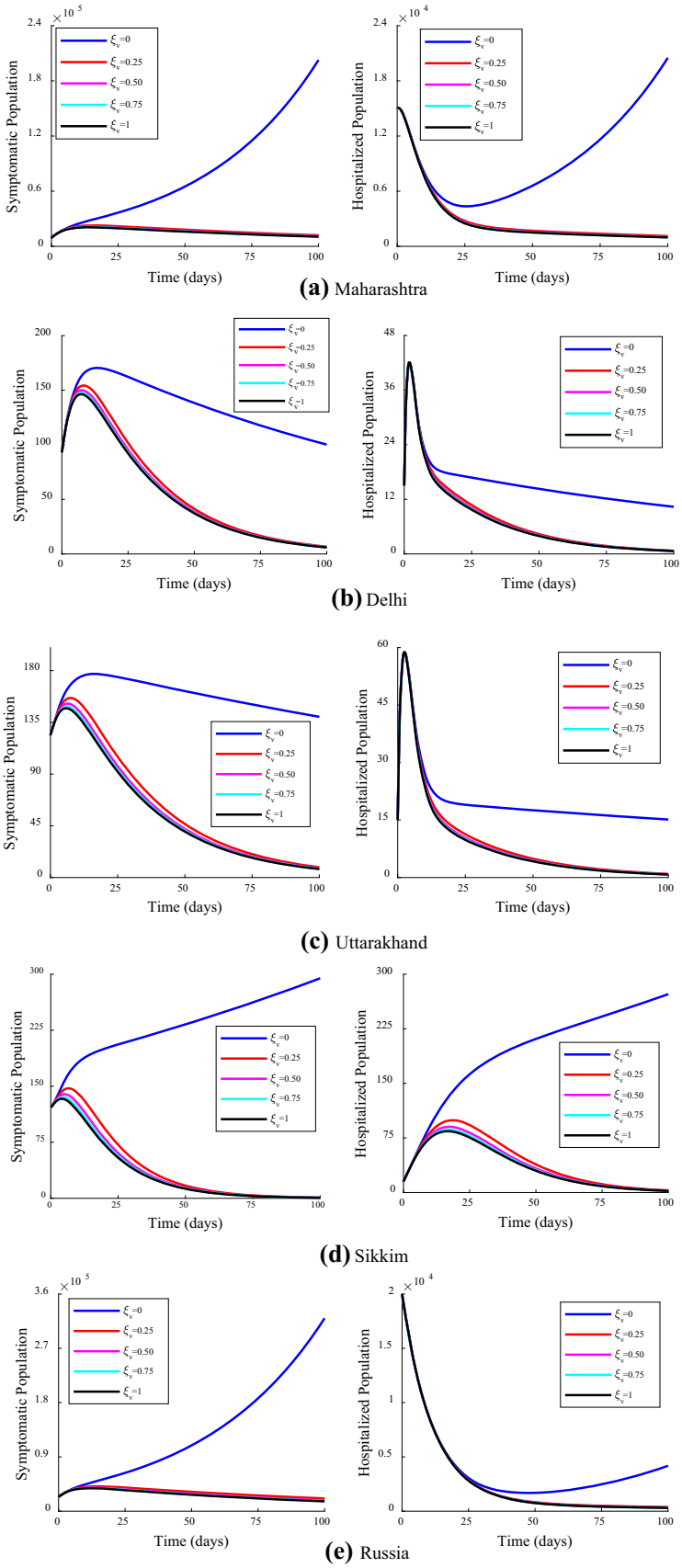

Fig. 4 Effect of vaccination

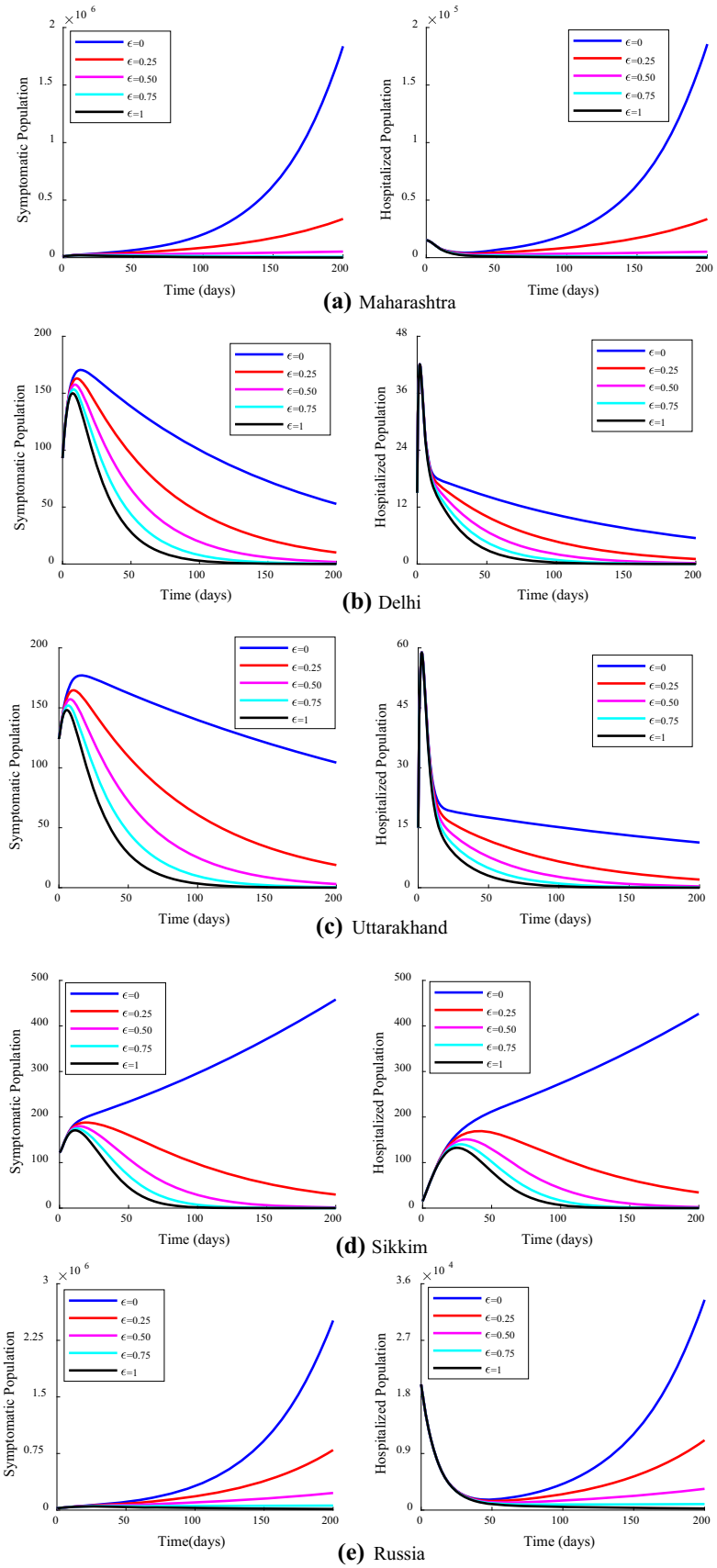

Fig. 5 Effect of vaccine efficacy

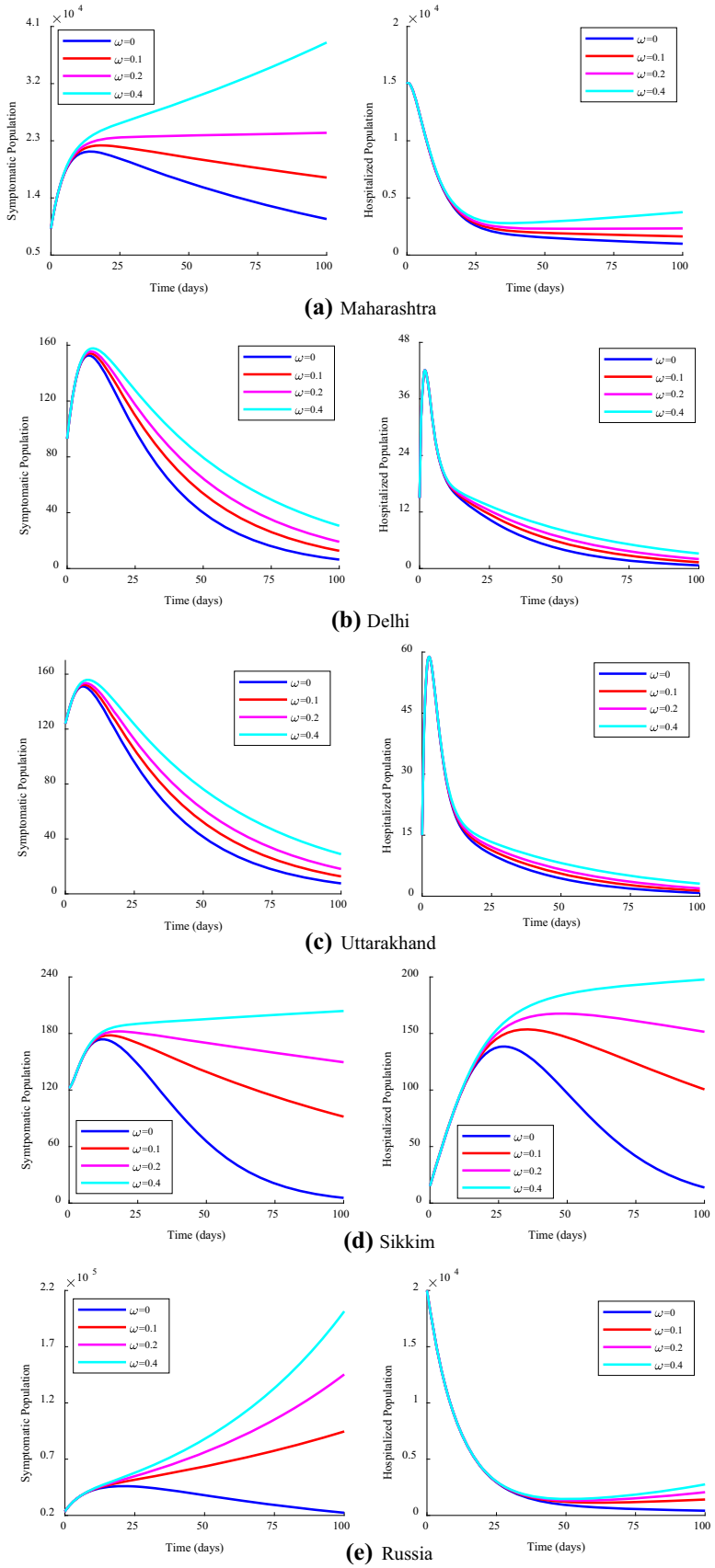

Fig. 6 Effect of vaccine-induced immunity

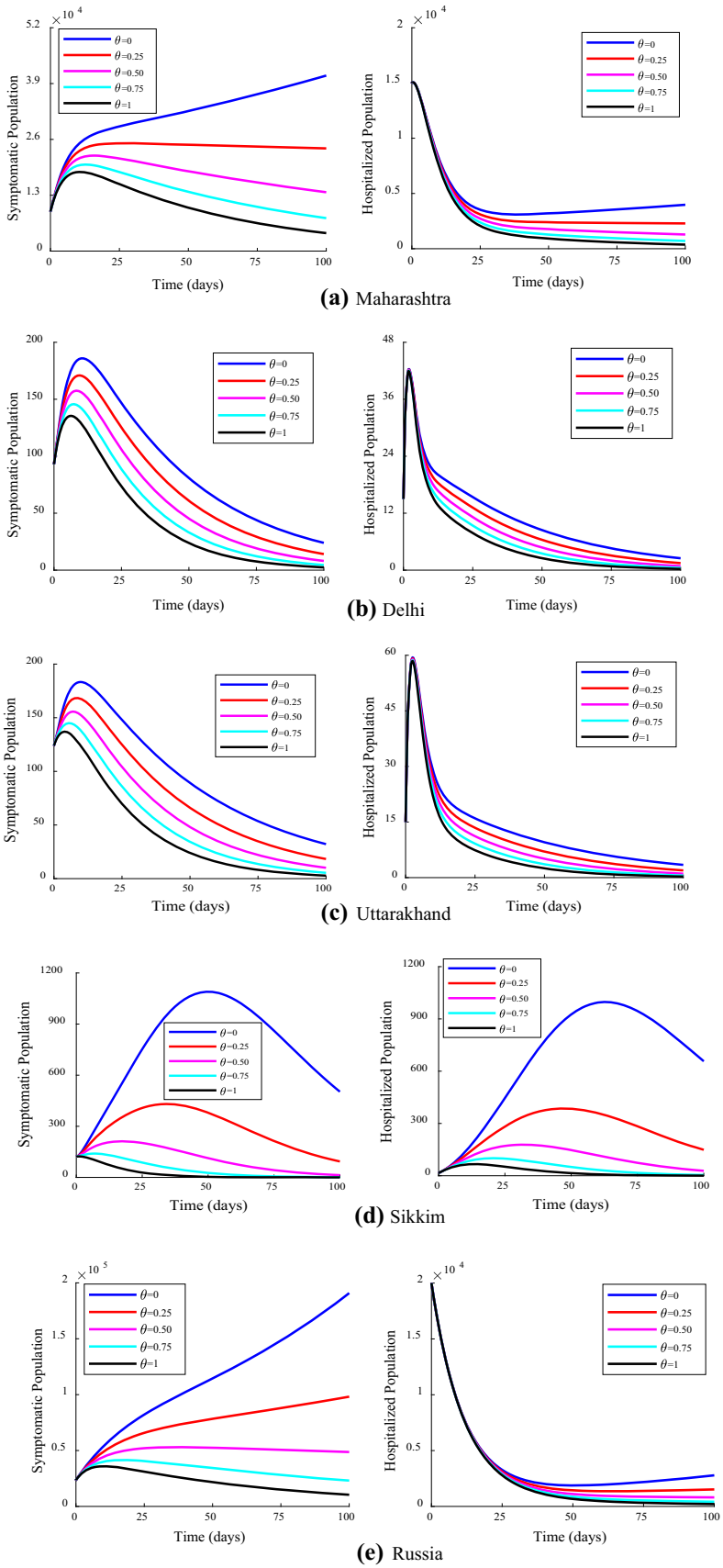

Fig. 7 Effect of lockdown

in all five regions. Whereas, an increase in vaccine-induced immunity results in a decrease in the number of symptomatic and hospitalized people.

6.5 The effect of lockdown

The portion of the population that follows the lockdown guidelines to guard each other from virus transmission has been measured by the parameter $\theta\,(0 \leq \theta \leq 1)$ known as the lockdown parameter. When $\theta = 0$, infers no lockdown guidelines have been implemented and people are freely shifting anywhere without any precaution, while $\theta = 1$ implies complete lockdown, which means total population is following COVID-19 guidelines such as wearing facemasks, maintaining social distance, and using sanitizers, which diminishes the number of droplets discharged into the environment by an infectious person. The variation in symptomatic and hospitalized cases in Maharashtra, Delhi, Uttarakhand, Sikkim, and Russia has been deliberated with the parameter θ. It is evident from Fig. 7 that there is depletion in the infection peak, as well as in the symptomatic and hospitalized populations, as the value of the parameter θ increases. Hence, for all five regions, it is determined that this parameter θ has a significant impact on the reduction of symptomatic and hospitalized populations. In particular, the low rate of the parameter θ drives the symptomatic and hospitalized cases to high values.

7 Conclusions and discussion

We introduced a nonlinear deterministic compartment model comprising a system of seven ordinary differential equations to perceive the COVID-19 transmission dynamics by incorporating a vaccination compartment. This model demonstrates COVID-19 dynamics from three distinct populations: symptomatic infected, asymptomatic infected, and vaccinated. Initially, to make our model epidemiologically and biologically feasible, basic properties like positivity of state variables and boundedness of solutions are derived. Further, the equilibrium points and the vaccine reproduction number of the proposed model are obtained using the next-generation matrix approach. The disease-free equilibrium point was shown to be locally and globally asymptotically stable whenever the corresponding vaccine reproduction number (R_{0v}) is smaller than unity. Similarly, the global stability of pandemic equilibrium point was verified whenever the corresponding vaccine reproduction number (R_{0v}) was greater than unity. In addition, extensive numerical simulations were executed to assess the impact of various control schemes (such as lockdown, vaccination, and treatment by drugs) on the spread of COVID-19 disease.

We calibrated proposed model parameters to fit daily mortality data from five regions: Maharashtra, Delhi, Uttarakhand, Sikkim, and Russia, from July 1st, 2021 to September 8th, 2021. From the data fitting in Fig. 2, it can be clearly visualized that model outputs are closely connected with the real data for all five regions. In addition, we computed the vaccine reproduction number to measure the disease transmission in the aforementioned regions. We asserted that the vaccine reproduction number is shorter than unity for Maharashtra, Delhi, Uttarakhand and Sikkim, while it is larger than unity for Russia, which means that the disease will soon be terminated in Indian states, while it shall remain in Russia. Afterwards, the consequences of pharmaceutical measures (such as treatment with drugs and vaccination) and non-pharmaceutical control measures (such as lockdown, wearing masks, usage of sanitizers, etc.) on COVID-19 infection are examined extensively. Along with these control measures, we investigated the significance of vaccine efficacy and vaccine-produced immunity in symptomatic and hospitalized cases. It was realized that pharmaceutical and non-pharmaceutical control policies could mitigate the symptomatic and hospitalized cases. In addition to the above, it was concluded that an upsurge in vaccine efficacy can curtail the infection. We detected that when vaccine efficacy is better, disease eradication is conceivable (Fig. 5). Furthermore, it was shown that by raising the vaccine-induced immunity period, the symptomatic and hospitalized COVID-19 cases shrank (Fig. 6). Finally, the outcome of lockdown is measured and it is found that a boost in the lockdown related parameter results in a decline in the corresponding symptomatic and hospitalized cases (Fig. 7).

In a nutshell, the current study suggests that all the COVID-19 intervention policies have a positive influence on the reduction of disease transmission in Maharashtra, Delhi, Uttarakhand, Sikkim, and Russia. Pharmaceutical and non-pharmaceutical control actions, as well as vaccine efficacy and vaccine-induced immunity, are critical to reduce COVID-19 prevalence in any region. Moreover, our results also specifies that vaccination of susceptible individuals and drug treatment of hospitalized individuals are significant in managing the COVID-19 pandemic in these regions. In fact, if a vaccine calamity arises, the government can majorly focus on drug treatment for hospitalized individuals rather than vaccination. This will undoubtedly mitigate disease transmission because it confers permanent immunity from disease. It is worth mentioning that our evaluation and conclusions are based on the current scenario of the pandemic in the aforementioned regions (COVID-19 second wave). Thus, we are hopeful that our established model and outcomes on the dynamics of COVID-19 will be beneficial for inspecting the disease dynamics in highly populated regions such as Russia, India, and China.

Author contribution statement

Each author has equally contributed to the paper.

References

1. C. Sohrabi, Z. Alsafi, N. O'neill, M. Khan, A. Kerwan, A. Al-Jabir, C. Losifidis, R. Agha, World Health Organization declares global emergency: a review of the 2019 novel coronavirus (COVID-19). Int. J. Surg. **76**, 71–76 (2020)
2. D. Cucinotta, M. Vanelli, WHO declares COVID-19 a pandemic. Acta. Biomed. **91**, 157–160 (2020)
3. F.A. Rabi, M.S. Al Zoubi, G.A. Kasasbeh, D.M. Salameh, A.D. Al-Nasser, SARS-CoV-2 and coronavirus disease 2019: what we know so far. Pathogens **9**, 231 (2020)
4. S.M. Garba, J.M.S. Lubuma, B. Tsanou, Modeling the transmission dynamics of the COVID-19 Pandemic in South Africa. Math. Biosci. **328**, 108441 (2020)
5. A.K. Singh, A. Misra, Impact of COVID-19 and comorbidities on health and economics: focus on developing countries and India. Diabetes Metab. Syndr. **14**, 1625–1630 (2020)
6. K. Thiagarajan, Why is India having a covid-19 surge? BMJ **373**, 1124 (2021)
7. S. Bugalia, V.P. Bajiya, J.P. Tripathi, M.T. Li, G.Q. Sun, Mathematical modeling of COVID-19 transmission: the roles of intervention strategies and lockdown. Math. Biosci. Eng. **17**, 5961–5986 (2020)
8. W.O. Kermack, A.G. McKendrick, A contribution to the mathematical theory of epidemics. Proc. R. Soc. A Math. Phys. Eng. Sci. **115**, 700–721 (1927)
9. R.M. Anderson, R.M. May, Population biology of infectious diseases: part I. Nature **280**, 361–367 (1979)
10. R.M. May, R.M. Anderson, Population biology of infectious diseases: part II. Nature **280**, 455–461 (1979)
11. E.V.M. dos Reis, M.A. Savi, A Dynamical Map to Describe Covid-19 Epidemics. Eur. Phys. J. Spec. Top. (2021)
12. Q. Lin, S. Zhao, D. Gao, Y. Lou, S. Yang, S.S. Musa, M.H. Wang, Y. Cai, W. Wang, L. Yang, D. He, A conceptual model for the coronavirus disease 2019 (COVID-19) outbreak in Wuhan, China with individual reaction and governmental action. Int. J. Infect. Dis. **93**, 211–216 (2020)
13. S.B. Bastos, D.O. Cajueiro, Modeling and forecasting the early evolution of the COVID- 19 pandemic in Brazil. Sci. Rep. **10**, 1–10 (2020)
14. M. Mandal, S. Jana, S.K. Nandi, A. Khatua, S. Adak, T.K. Kar, A model-based study on the dynamics of COVID-19: prediction and control. Chaos Solit. Fract. **136**, 109889 (2020)
15. R.K. Rai, S. Khajanchi, P.K. Tiwari, E. Venturino, A.K. Misra, Impact of social media advertisements on the transmission dynamics of COVID-19 pandemic in India. J. Appl. Math. Comput. **68**, 19–44 (2022)
16. A. Gowrisankar, L. Rondoni, S. Banerjee, Can India develop herd immunity against COVID-19? Eur. Phys. J. Plus. **135**, 526 (2020)
17. D. Easwaramoorthy, A. Gowrisankar, A. Manimaran, S. Nandhini, L. Rondoni, S. Banerjee, An exploration of fractal-based prognostic model and comparative analysis for second wave of COVID-19 diffusion. Nonlinear Dyn. **106**, 1375–1395 (2021)
18. C. Kavitha, A. Gowrisankar, S. Banerjee, The second and third waves in India: when will the pandemic be culminated? Eur. Phys. J. Plus. **136**, 596 (2021)
19. S. Khajanchi, K. Sarkar, S. Banerjee, Modeling the dynamics of COVID-19 pandemic with implementation of intervention strategies. Eur. Phys. J. Plus. **137**, 129 (2022)
20. P. Das, R.K. Upadhyay, A.K. Misra, F.A. Rihan, P. Das, D. Ghosh, Mathematical model of COVID-19 with comorbidity and controlling using non-pharmaceutical interventions and vaccination. Nonlinear Dyn. **6**, 1213–1227 (2021)
21. B.H. Foy, B. Wahl, K. Mehta, A. Shet, G.I. Menon, C. Britto, Comparing COVID-19 vaccine allocation strategies in India: a mathematical modelling study. Int. J. Infect. Dis. **103**, 431–438 (2021)
22. J.P. La Salle, *The stability of dynamical systems*. Regional Conference Series in Applied Mathematics. SIAM, Philadelphia (1976)
23. P.S. Rana, N. Sharma, Mathematical modeling and analysis with various parameters, for infection dynamics of Tuberculosis. J. Phys. Conf. Ser. **1504**, 012007 (2020)
24. Covid-19 India, Maharashtra (2021). https://www.covid19india.org/state/MH
25. Covid-19 India, Delhi (2021). https://www.covid19india.org/state/DL
26. Covid -19 India, Uttarakhand (2021). https://www.covid19india.org/state/UT
27. Covid -19 India, Sikkim (2021). https://www.covid19india.org/state/SK
28. Coronavirus Russia, worldometer (2021). https://www.worldometers.info/coronavirus/country/russia/
29. C.N. Ngonghala, E.A. Iboi, A.B. Gumel, Could masks curtail the post-lockdown resurgence of COVID-19 in the US? Math. Biosci. **329**, 108452 (2020)
30. India Census, Maharashtra Population (2021). https://www.indiacensus.net/states/maharashtra
31. I. Ghosh, M. Martcheva, Modeling the effects of prosocial awareness on COVID-19 dynamics: case studies on Colombia and India. Nonlinear Dyn. **104**, 4681–4700 (2021)
32. E. Michael, K. Newcomb, A. Mubayi, I. Mahmood. Recovery from the COVID-19 pandemic by mass vaccination: emergent lessons from the United States and India. MedRxiv (2021). https://doi.org/10.1101/2021.05.26.21257847
33. A.K. Srivastav, P.K. Tiwari, P.K. Srivastava, M. Ghosh, Y. Kang, A mathematical model for the impacts of face mask, hospitalization and quarantine on the dynamics of COVID-19 in India: deterministic vs. stochastic. Math. Biosci. Eng. **18**, 182–213 (2021)
34. Demographics India, worldometer (2021). https://www.worldometers.info/demographics/india-demographics/#life-exp
35. S. Umakanthan, S. Patil, N. Subramaniam, R. Sharma, COVID-19 vaccine hesitancy and resistance in India explored through a population-based longitudinal survey. Vaccines **9**, 1064 (2021)
36. R. Li, S. Pei, B. Chen, Y. Song, T. Zhang, W. Yang, J. Shaman, Substantial undocumented infection facilitates the rapid dissemination of novel coronavirus (SARS-CoV-2). Science **368**, 489–493 (2020)

37. S. Pal, I. Ghosh, A mechanistic model for airborne and direct human-to-human transmission of COVID-19: effect of mitigation strategies and immigration of infectious persons. Eur. Phys. J. Spec. Top. (2022)
38. India Census, Delhi Population (2021). https://www.indiacensus.net/states/delhi
39. India Census, Uttarakhand Population (2021). https://www.indiacensus.net/states/uttarakhand
40. India Census, Sikkim Population (2021). https://www.indiacensus.net/states/sikkim
41. Population Russia, worldometer (2021). https://www.worldometers.info/world-population/russia-population/
42. K.N. Nabi, Forecasting COVID-19 pandemic: a data-driven analysis. Chaos Solit. Fract. **139**, 110046 (2020)
43. M. Al-Raeei, M.S. El-Daher, M.S. and O. Solieva, Applying SEIR model without vaccination for COVID-19 in case of the United States, Russia, the United Kingdom, Brazil, France, and India. Epidemiol. Methods. 10 (2021)
44. Demographics Russia, worldometer (2021). https://www.worldometers.info/demographics/russia-demographics/
45. I. Jones, P. Roy, Sputnik V COVID-19 vaccine candidate appears safe and effective. The Lancet **397**, 642–643 (2021)
46. K.C. Samal, B. Panda, L. Behera, Anti-Covid Drug: 2-deoxy-D-glucose and its mechanism of action. Biotica Res Today **3**, 345–347 (2021)
47. S. Balsari, Z. Udwadia, A. Shaikh, A. Ghafur, S. Kataria, Contextualising evidence-based recommendations for the second wave of the COVID-19 pandemic in India. Lancet Infect. Dis. **21**, 905–907 (2021)